Journal of Multidisciplinary Engineering Science and Technology (JMEST)
ISSN: 2458-9403
Vol. 6 Issue 9, September - 2019

# Effect of Co nano-particales doping on polycrystalline YBCO123 high temperature superconductor

**Abdul Rhman Rajab Ali Nefrow**
Department of Physics, Faculty of Arts and Science, Elmergib University
Al Khums City, Libya
e-mail: abdulnefrow09@gmail.com

**Mohammed Rajab Ali Alqiddar, and Khaled Ibrahim Ali**
Department of Physics, Faculty of Science,
Al Asmarya Islamic University, Zliten City, Libya

***Abstract*— Bulk superconductor samples of $YBa_2Cu_{3-x}Co_xO_{7-\delta}$ with (x= 0.0, 0.1, 0.15 wt%) are synthesized by solid-state reaction method. Both x-ray diffraction (XRD) and electron microscopy have been employed to study the phase identification, dislocations and the local structure of these samples. Transition temperature of the samples has been determined by four probe resistance measurements. The x-ray diffraction patterns indicate that the gross structure of $YBa_2Cu_{3-x}Co_xO_{7-\delta}$ do not change with the substitution of Co. The zero resistance critical transition temperature ($T_c$) is found to decrease with the increase concentration of Co in compound.**

***Keywords*— YBCO; Y123; solid state reaction method; Co doping.***

## I. INTRODUCTION

Since the discovery of the YBCO compound system, a large number of researchers have conducted studies on the investigation and development of superconducting properties. A number of articles have been published to investigate the superconductivity and structural properties of YBCO samples. Many groups have made adding or substitution for developing the properties of the Y123. Gupta et al. [1] made Co doping to Y123 system; lattice parameters increases with the contribution and critical temperature value has been increased with the increasing of the Co doping. Roa et al. [2] published their results by applying the stress-strain test on Y123 superconducting ceramic structures. The compatibility of the results of this study with the literature is discussed. In another study on B-doped Y123, Ben Azzouz et al. [3] stated that this doping reduced the critical temperature value and that the lattice parameters changed with boron substitution. Similarly, Volochova et al. [4] investigated the effect of Sm and Y on the critical temperature of Y123. Özturk et al. [5] examined the characteristics of the Lu-doped Y123 structure and reported that they increased the critical current density when 50% Lu was doped to the Y123 structure. Dadras et al. [6] in their study in 2016, they doped Au nanoparticle to Y123 phase. In the study sol-gel method used and it was emphasized that Au nanoparticle doping increased critical temperature value and decrease particle size. In this study where magnetic properties were examined, 1% contribution rate was determined as optimum. Hamrita et al. [7] in 2014, compared the ball milling to hand milling for producing the Y123 phase superconductor. When the critical temperature values are examined; it is concluded that the hand milled sample has a higher critical temperature value than the samples produced by ball milling at different rotational speeds or at different ball numbers. Slimani et al. [8] in the Y123 system in which they studied their properties by adding $CoFe_2O_4$ in 2014, they discussed structural changes of the lattice parameters and surface morphology. In this study, they showed that $CoFe_2O_4$ addition affects the superconductivity properties and proof that critical temperature value decreases with the addition of $CoFe_2O_4$.

In this study, we produced the samples with conventional solid state reaction method and substituted Co nanoparticle with Cu. We aimed to investigate the structural, morphological and superconducting properties of the Co doped Y123 system.

## II. EXPERIMENTAL

In this study, superconductor materials in Y123 phase were prepared by conventional solid state reaction method. $Y_2O_3$ (Yttrium (III) oxide %99.99, Alfa Aesar), $BaCO_3$ (Barium carbonate %99.95, Alfa Aesar), CuO (Copper (II) oxide %99.9995, Alfa Aesar) and Co-nanoparticle (Cobalt powder-325 mesh %99.5, Alfa Aesar) powders were used in the sample preparation. The required weighted powders were ground in agate mortar for 1 hour and put into alumina boats. Samples calcined at 850°C for 24 hours in Protherm PLT-120/5 model ash furnace. Calcination process repeated 3 times and after each calcination powders grounded in agate mortar for 1 hour. After the third calcination process, grounded powders form into 13 mm diameter and 2 mm thickness bulk by using cold press. The tablet samples were placed in Protherm PTF-15/45/450 model tube furnace on the alumina crucible and sintering process applied. Samples sintered at 930°C for 24 hours by heating rate of 5°C/min and then cooled to 500°C in 60 minutes. The samples were kept in the oxygen atmosphere for 5 hours at 500°C. Samples are named as Y123-U, Y123-10 and Y123-15 in accordance with doping ratio.

The phase diagnosis and structural analysis were investigated by Bruker D8 Advance X-ray

diffractometer in the range of 2θ=3-90° with CuKα. Surface morphology and elemental analysis investigated by FEI Quanta Feg 250 model scanning electron microscopy. Electrical resistance measurements performed by conventional four probe method.

## III. Results and Discussion

The XRD patterns of all samples produced in $Y_1Ba_2Cu_{3-x}Co_xO_{7-\delta}$ general formula with the x = 0, 0.10 and 0.15 doping ratios are given in Fig 1. When XRD patterns were examined, it was seen that peaks indicated by miller indices were peaks of Y123 phase. The fact that Co peaks were not found in XRD patterns showed that Co atoms entered into orthorhombic Y123 structure by doping process. The displacement of $Co^{+3}$ (ionic radius 0.745 Å) with $Cu^{+2}$ (ionic radius 0.73 Å) played an important role in the introduction of Co atoms as a result of the doping process. Co atoms entering the structure caused some changes in peak intensity but did not corrupt orthorhombic structure.

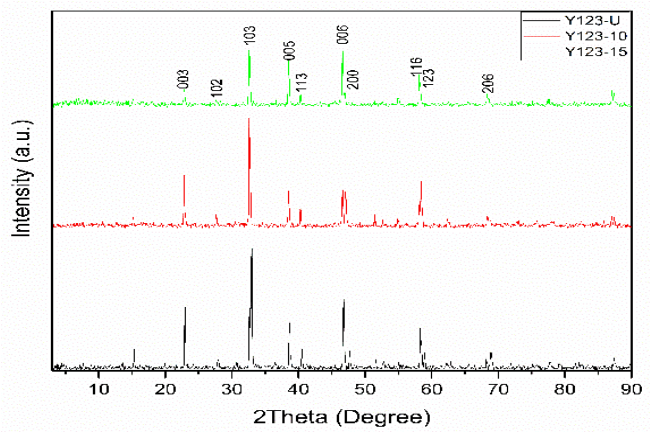


Fig. 1. XRD patterns and miller indices of produced samples

Since Y123 is an orthorhombic structure; d the distance between the planes and the data such as the a, b, and c parameters were calculated by formula;

$$\frac{1}{d^2} = \frac{h^2}{a^2} + \frac{k^2}{b^2} + \frac{l^2}{c^2} \quad (1)$$

using the indices h, k, l from the XRD. Grain size, D, calculated using formulas;

$$D = 0.941\lambda / B\cos\theta \quad (2)$$

$$B^2 = B_s^2 - B_m^2 \quad (3)$$

here $B_s$ is the full width half of maximum (FWHM) and $B_m$ is 0.000007 [9].

In the literature, the lattice parameters of Y123 structure are given as a=3.82 Å, b=3.89 Å and c=11.7 Å respectively. It is seen that the lattice parameters of Y123 for superconducting samples with Co doping produced using solid state reaction method are in accordance with the literature. The grain size values given in Table 1 show that the particle size increases with the increase of Co doping.

Table 1. Lattice parameters and particle size values

| *Sample* | *Grain Size (Å)* | *a (Å)* | *b (Å)* | *c (Å)* |
|---|---|---|---|---|
| Y123-U | 28.95 | 3.815 | 3.882 | 11.683 |
| Y123-10 | 37.63 | 3.822 | 3.884 | 11.687 |
| Y123-15 | 38.13 | 3.826 | 3.879 | 11.691 |

SEM analysis was performed to determine the particle boundaries, inter-particle distance and particle size of Co doped samples obtained by solid state reaction method. Fig 2 contains the SEM images of the samples. In Fig 2 large images were taken at 2500 magnification, while internal pictures were taken at 10000 magnification. From the SEM images, it is seen that the particle sizes increase with Co contribution. This change is in agreement with the particle size values calculated by XRD results. The variation of particle boundaries and inter-particle distance is clearly seen in Fig 2. In addition, the increased particle size with the doping also led to a decrease in porosity.

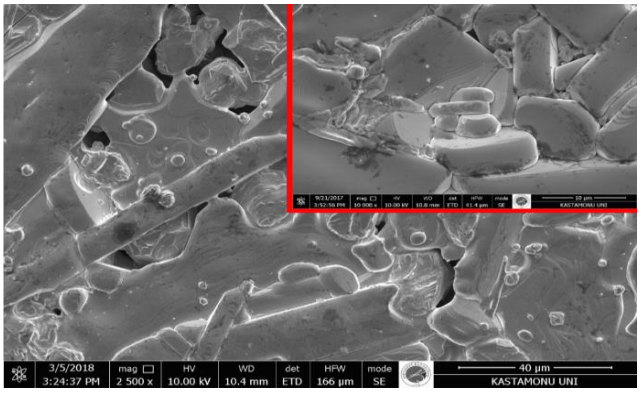


(a)

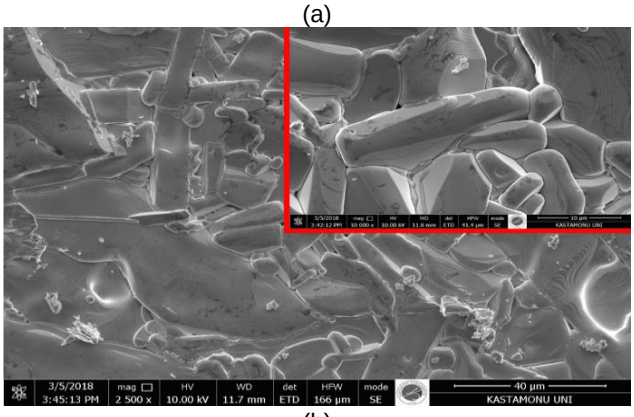


(b)

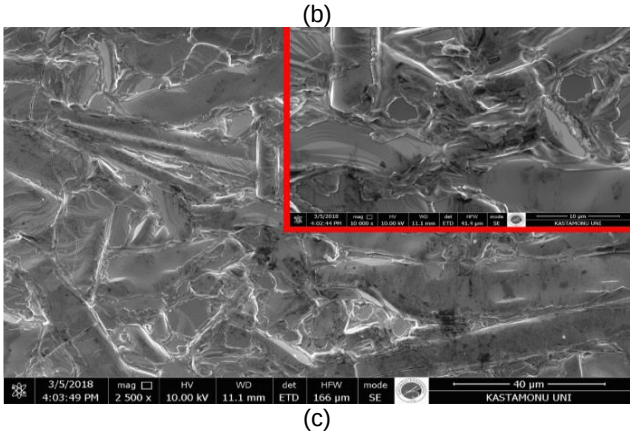


(c)

Fig. 2. SEM IMAGES OF SAMPLES PRODUCED BY SOLID STATE REACTION METHOD (A; Y123-U, B; Y123-10, C; Y123-15)

The graphic obtained from the EDS spectrum is a graph of intensity versus energy. In these results, there is a linear ratio between the atomic amount and the intensity of the graph. By EDS analysis, the weight ratios of the atoms in the sample can be obtained. It is also possible to determine whether or not impurities are present in the material with EDS. The EDS results given in Fig 3, clearly show that the Co doping rate increases as calculated and the Cu ratio is reduced. Thus, it can be concluded that there is a displacement between the Co and Cu ions in the targeted manner.

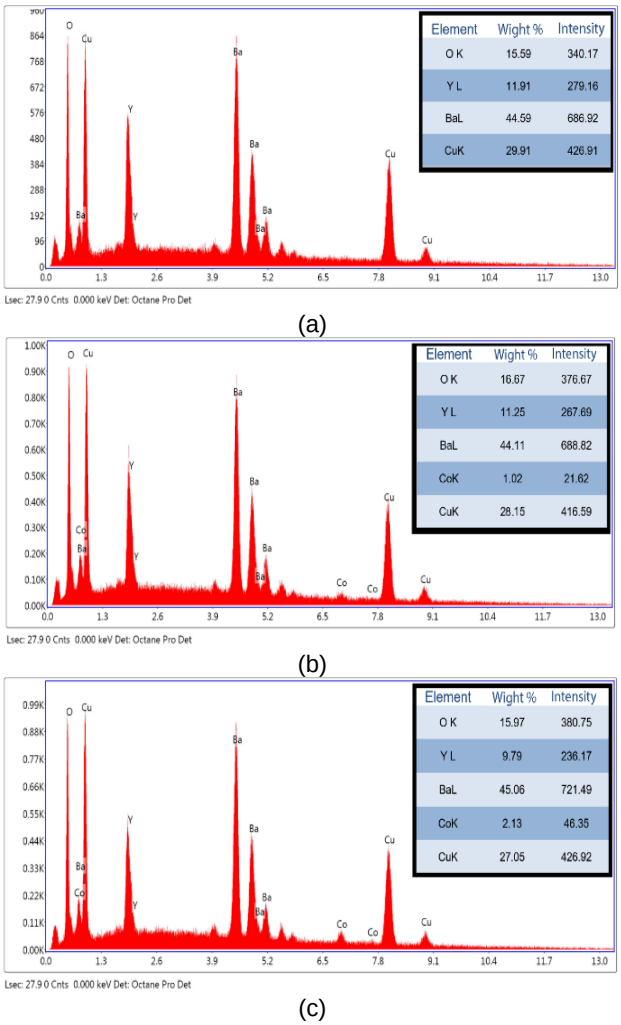


Fig. 3. EDS RESULTS OF SAMPLES PRODUCED BY SOLID STATE REACTION METHOD (A; Y123-U, B; Y123-10, C; Y123-15)

Electrical resistance (R-T) measurements versus temperature inform us about the behavior of materials at low temperatures. The electrical measurement results of the Co doped samples produced by solid-state reaction method are given in Fig 4. As a result of electrical resistance measurements, all samples produced in this group have superconductive properties. With this result, it was supported that the Co atoms entering the structure did not disturb the orthorhombic structure. The critical temperature value of the material decreased with the increase of the doping ratio. The values obtained from this measurement are given in Table 2.

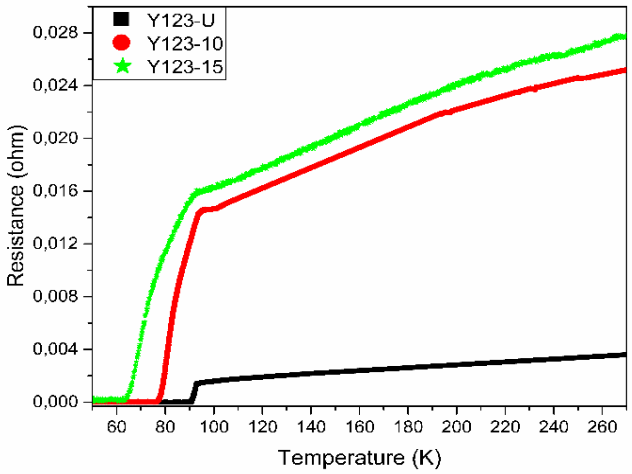


Fig. 4. R-T RESULTS OF SAMPLES PRODUCED BY SOLID STATE REACTION METHOD

TABLE 2. VALUES OBTAINED FROM R-T MEASUREMENT

| *Samples* | *Critical Temperature (K)* | | $\Delta T_C(K)$ |
|---|---|---|---|
| | $T_C^{onset}$ | $T_C^{offset}$ | $T_C^{onset}$-$T_C^{offset}$ |
| *Y123-U* | *92.96* | *90.29* | *2.67* |
| *Y123-10* | *92.68* | *76.63* | *16.05* |
| *Y123-15* | *91.75* | *63.43* | *28.32* |

The highest transition temperature and the lowest superconductivity transition range ($\Delta T_C$) value are in the undoped sample. With the increase of the doping ratio, the transition temperature decreased while the superconductivity transition interval increased. At the same time, room temperature resistance also increased with the doping ratio. It is stated that this is caused by the Co atoms entering the structure to increase the resistance of the particle boundaries of the structure [10].

## IV. CONCLUSION

In the study, the solid-state reaction method which is widely used in the production of high-temperature superconducting samples has been used. XRD, SEM, EDS and R- measurements are performed for all samples to investigate structural, morphologic and superconducting properties.

In the XRD results, it was observed that the peaks shifted to the low angle values in direct proportion to the doping ratio. It is predicted that this may be due to the tendency to disrupt the orthorhombic structure. In addition, the decrease in peak intensity with the doping indicates that the crystallinity has deteriorated. From the SEM images it was observed that, surface morphology changed with doping. Increasing of doping ratio increased the porosity of the samples surface. Electrical resistance measurements showed that all samples have affected by doping. Increasing of Co ratio deceased the transition temperature of Y123 phase.

## REFERENCES

[1] S. Gupta, R.S. Yadav, N.P. Lalla, G.D. Verma, and B. Das, “Microstructural and

Superconducting Properties of $YBa_2Cu_{3-x}Co_xO_{7-\delta}$ System," Integrated Ferroelectrics, 116:1, pp. 68-81, 2010.

[2] J.J. Roa, E. Jiménez-Piqué, X.G. Capdevila, and M. Segarra, "Nanoindentation with spherical tips of single crystals of YBCO textured by the Bridgman technique: Determination of indentation stress–strain curves," Journal of the European Ceramic Society, 30, pp. 1477–1482, 2010.

[3] F. Ben Azzouz, M. Zouaoui, K.D. Mani, M. Annabi, G. Van Tendeloo, and M. Ben Salem, "Structure, microstructure and transport properties of B-doped YBCO system," Physica C: Superconductivity and its Applications, 442, pp. 13–19, 2006.

[4] D. Volochova, K. Jurek, M. Radusovska, S. Piovarci, V. Antal, J. Kovac, M. Jirsa, and P. Diko, "Contamination of YBCO bulk superconductors by samarium and ytterbium," Physica C: Superconductivity and its Applications, 496, pp. 14–17, 2014.

[5] A. Öztürk, I. Düzgün, and S. Çelebi, "The effect of partial Lu doping on magnetic behaviour of YBCO (123) superconductors," Journal of Alloys and Compounds, 495, pp. 104–107, 2010.

[6] S. Dadras, and Z. Gharehgazloo, Effect of Au nano-particles doping on polycrystalline YBCO high temperature superconductor," Physica B: Condensed Matter, 492, pp. 45–49, 2016.

[7] A. Hamrita, Y. Slimani, M.K. Ben Salem, E. Hannachi, L. Bessais, F. Ben Azzouz, and M. Ben Salem, "Superconducting properties of polycrystalline $YBa_2Cu_3O_{7-\delta}$ prepared by sintering of ball-milled precursor powder," Ceramics International, 40, pp. 1461–1470, 2014.

[8] Y. Slimani, E. Hannachi, M.K. Ben Salem, A. Hamrita, A. Varilci, W. Dachraoui, M. Ben Salem, and F. Ben Azzouz, "Comparative study of nano-sized particles $CoFe_2O_4$ effects on superconducting properties of Y-123 and Y-358. Physica B: Condensed Matter, 450, pp. 7–15, 2014.

[9] B.D. Josephson, "Possible new effects in superconductive tunneling," Physics Letters, 1, 7, pp. 251-253, 1962.

[10] T. Metin, and M. Tepe, "The effect of Ag doping on the sıperconducting properties of $Y_3Ba_5Cu_{8-x}Ag_xO_{18-\delta}$ ceramics," Journal of Superconductivity and Novel Magnetism., 30(4), pp. 1083-1087, 2016.